

1

*Parsing spatio-temporal behaviour of dyads*

2

A relative-motion method for parsing spatio-temporal behaviour of dyads

3

using GPS relocation data

4

Ludovica Luisa Vissat<sup>1</sup>, Jason K. Blackburn<sup>2,3</sup>, Wayne M. Getz<sup>1,4,\*</sup>

5

<sup>1</sup>*Dept. ESPM, University of California, Berkeley, 130 Hilgard Way, Berkeley, CA 94720-3114, USA*

6

<sup>2</sup>*Spatial Epidemiology and Ecology Res. Lab., Department of Geography, University of Florida, 330 Newell*

7

*Dr, Gainesville, FL 32611, USA*

8

<sup>3</sup>*Emerging Pathogens Institute, University of Florida, 2055 Mowry Road, Gainesville, FL 32610, USA*

9

<sup>4</sup>*School of Mathematical Sciences, University of KwaZulu-Natal, 238 Mazisi Kunene Rd, Glenwood,*

10

*Durban, 4041, South Africa*

11

*\*Corresponding author: [wgetz@berkeley.edu](mailto:wgetz@berkeley.edu)*

## 12 **Abstract**

13 1. In this paper, we introduce a novel method for classifying and computing the frequencies of movement  
14 modes of intra and interspecific dyads, focusing in particular on distance-mediated approach, retreat, fol-  
15 lowing and side by side movement modes.

16 2. Besides distance, the method includes factors such as sex, age, time of day, or season that cause frequen-  
17 cies of movement modes to deviate from random.

18 3. We demonstrate and validate our method using both simulated and empirical data. Our simulated data  
19 were obtained from a relative-motion, biased random-walk (RM-BRW) model with attraction and repulsion  
20 circumferences. Our empirical data were GPS relocation time series collected from African elephants in  
21 Etosha National Park, Namibia. The simulated data were primarily used to validate our method while the  
22 empirical data analysis were used to illustrate the types of behavioral assessment that our methodology  
23 reveals.

24 4. Our methodology facilitates automated, observer-bias-free analysis of the locomotive interactions of dyads  
25 using GPS relocation data, which is becoming increasingly ubiquitous as telemetry and related technologies  
26 improve. Our method should open up a whole new vista of behavioral-interaction type analyses to movement  
27 and behavioral ecologists.

28 *Keywords:* African elephant, approach and retreat, biased random walk, dyadic interactions, *Loxodonta*  
29 *africana*

## 30 **1. Introduction**

31 Most studies of dyadic interactions involve making observations of individuals at close quarters (White-  
32 head and Dufault, 1999); for example, agonistic interactions in social insects (Getz and Smith, 1986, Breed,  
33 2003), grooming networks in primates (Voelkl et al., 2011), and dominance behavior in elephants (Archie  
34 et al., 2006, Wittemyer and Getz, 2007). An exception though are a new class of methods that use global  
35 positioning system (GPS) telemetry data to assess the joint movement of individuals that may be some  
36 distance apart and not simultaneously directly observable to a visual recorder (human or camera) (Joo  
37 et al., 2018). Of course, the assumption is that individuals not in visual contact with one another may still  
38 have auditory (Hulse, 2002, Erbe et al., 2016), olfactory (Shorey, 2013), or even low frequency vibratory  
39 cues (McComb et al., 2003, O’Connell-Rodwell, 2007) regarding the location of other individuals within a  
40 radius and direction salient to the perceptual modality involved (with wind direction playing a critical role  
41 in olfactory communication).

42 In this paper, we continue to develop the opportunities for evaluating dyadic movement interactions  
43 using GPS relocation data by presenting a technique that allows us to classify dyadic modes of movement  
44 in terms of distance-dependent approach, retreat, following, and side by side modes of movement. Other  
45 salient factors such as the sexes and ages of the individuals, the time of day or year, the internal state of the  
46 individuals and the state of the environment may also be included in an extended version of our method.  
47 Specifically, our method is based on the analysis of pairs of animal trajectories with overlapping time periods,  
48 comparable frequencies and without major gaps in the data collection. By considering individual directions  
49 and locations, our approach allows us to extract both individual and dyadic behaviors, whether symmetric  
50 (e.g., both individual moving towards each other) or asymmetric (e.g., one advancing and one retreating).  
51 This new methodology extends existing analysis: it allows us to understand details of dyad interactions by  
52 classifying different behaviour types and grouping the results based on distance apart, which can be up to  
53 several kilometers for individuals using auditory communication (McComb et al., 2003, O’Connell-Rodwell,  
54 2007).

55 In the case of two individuals moving in the same general direction, whether they are moving side by  
56 side or one is pursuing the other will come down to an assessment based on relative speeds and headings,  
57 and, ultimately, the terminal behavior at the end of the event or even the identity of the individuals involved  
58 (e.g., two predators pursuing the same unknown prey versus a predator pursuing a known prey).

59 Since our method is novel, we need to demonstrate both its validity and its utility. We undertake  
60 the former by applying our method to simulated data with known dyadic interactions to see how well the  
61 method uncovers these interactions embedded in movement data. We undertake the latter by analysing  
62 GPS data obtained from GPS collared African elephants (*Loxodonta africana*), in Etosha National Park,  
63 Namibia (Abrahms et al., 2017, Tsalyuk et al., 2019). Our simulation data are generated by a novel relative-  
64 motion, biased random-walk (RM-BRW) model with attraction and repulsion circumferences constructed and  
65 implemented using the Numerus Model Builder (NMB) simulation platform (Getz et al., 2018). Although  
66 we use our simulation data to demonstrate the ability of our method to correctly identify known behaviors  
67 embedded in the model, it can also be used to test various hypotheses about the structure of empirical data,  
68 particularly in the context of evaluating whether or not particular movement patterns differ significantly  
69 from patterns that may be generated at random.

70 In the rest of this paper, in Section 2 we first introduce our general method and we next report details of  
71 the method’s implementation. This is followed by our description of the model used to generate simulated  
72 data and a description of our empirical data. We then present a report in Section 3 of the application of

73 our method to the simulated and to the empirical data. Finally, we present a discussion of related work in  
74 Section 4 and then end with concluding remarks in Section 5.

## 75 **2. Materials and Methods**

### 76 *2.1. Method*

77 We developed our method to study, in particular, how approach and retreat behavior in pairs of individ-  
78 uals may depend on the current distance between them, using locations recorded at the same, or close to  
79 the same, times. Since direction of movement and speed are needed to classify the different behaviour types,  
80 consecutive relocation points are needed of the type obtained using GPS telemetry data (Calenge et al.,  
81 2009). In addition, the frequency of location sampling should be sufficiently high to ensure that estimates of  
82 direction and speed are relevant to the scale of the analysis (Codling and Hill, 2005). GPS collar battery life  
83 creates a trade-off between the frequency of GPS point collection and the total tracking period for an animal.  
84 The empirical study undertaken here includes data in the 15-30 minute sampling range, which is frequently  
85 reported in terrestrial animal movement studies. Hence this range will be the focus of our discussion.

86 To begin, the relocation data from pairs of individuals are time-matched so that consecutive relocation  
87 points obtained from these individuals can be used to compute heading directions and speed for each.  
88 Although these computed directions and speeds for each individual may not be perfectly matched in time,  
89 they are nominally labeled as occurring at common times  $t$ ,  $t + 1$ ,  $t + 2$ , and so on if deviations from these  
90 times are sufficiently small compared to the size of inter-sampling interval: e.g., if points in both relocation  
91 sets are collected every 15 minutes, then we may decide that points collected in different sets within a  
92 threshold of 2 or 3 minutes of one another can be matched up, where this threshold may be varied to see  
93 how results are affected. Our method then proceeds by a considering time series vector set  $\mathcal{T}$  containing the  
94 following information at each time point  $t$  regarding two individuals labeled A and B and their positions at  
95 time  $t$  and  $t + 1$ : viz., the absolute headings ( $\text{headA}$ ,  $\text{headB}$ ), the relative headings ( $\text{dirAB}$ ,  $\text{dirBA}$ ) (which  
96 we define as direction towards the other individual in the dyad), the difference between absolute and relative  
97 headings ( $\text{diffA}$ ,  $\text{diffB}$ ), the speed ( $s_A$ ,  $s_B$ ), and the pair distance ( $d_{AB}$ ). Either some or all of these values  
98 will be used in the different analysis (individual, dyadic, extended) proposed in this paper. Thus our time  
99 series is:

$$\mathcal{T} = \left\{ \left( \text{headA}(t), \text{headB}(t), \text{dirAB}(t), \text{dirBA}(t), \text{diffA}(t), \text{diffB}(t), s_A(t), s_B(t), d_{AB}(t) \right) \middle| t = 0, \dots, T - 1 \right\}$$

100 In the following, we describe how we compute the entries for individual A with respect to individual B.  
 101 For the  $t^{\text{th}}$  entry in  $\mathcal{T}$ , this computation requires the positions of A and B at time  $t$  and A at time  $t + 1$ ,  
 102 which we denote by  $A(t)$ ,  $B(t)$  and  $A(t + 1)$  (Fig. 1, left panel).

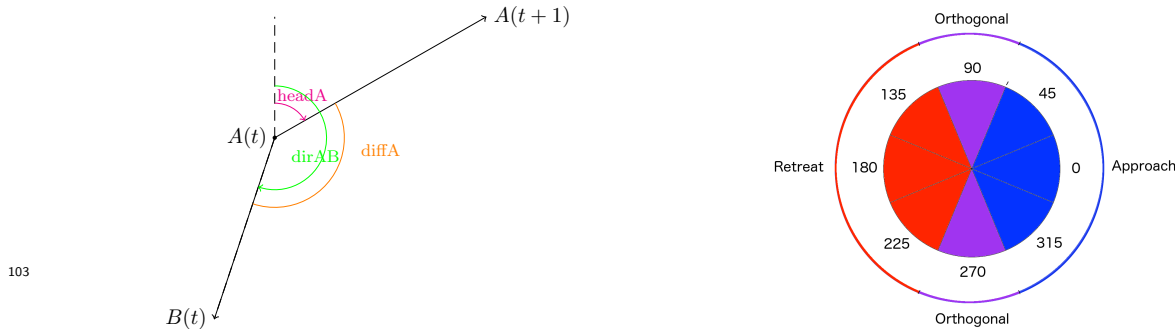


Figure 1: Left panel: absolute heading (**headA**), relative heading (**dirAB**) and difference between these two angles (**diffA**) for individuals A in relation to individual B. Right panel: classification of absolute value of the difference among the individual absolute and relative heading, based on an 8 equal tranche segmentation of the unit circle (numbers represent the central angle value of each tranche, where  $0 \equiv 360$ ). Other levels of segmentation, say twelve, can be used and results obtained can be compared for sensitivity of the results obtained to a more demanding scale of segmentation (in the 12 segment case, the purple areas encompasses two 30 rather than 45 degree tranches). Blue represents **approach** behaviour, red represents **retreat** behaviour while purple represents **orthogonal** behaviour.

104 In calculating angles (e.g., **headA**, **dirAB** and **diffA** for individual A), we use the convention that north is  
 105 0 and measure clockwise, following the convention used by the function **bearing** in the R package **geosphere**.  
 106 The speed of individual A at time  $t$  is calculated as the ratio of the distance  $d(A(t), A(t + 1))$  and the time  
 107 interval between  $t$  and  $t + 1$ . The entry  $d_{AB}$  is the pair distance  $d(A(t), B(t))$ . The values of the first two  
 108 calculated angles (e.g., **headA** and **dirAB** for individual A) lie in  $[0, 360)$  and therefore the absolute value  
 109 of their difference (e.g., **diffA** for individual A) lies in the same interval. We divide the turning circle into  
 110 8 sections (Fig. 1, right panel), and consider individual A to be *approaching* individual B if **diffA** is below  
 111 67.5 or above 292.5 (area shown in blue), while if **diffA** is between 112.5 and 247.5 (area shown in red) A  
 112 is considered to be *retreating* from B. If **diffA** lies between 67.5 and 112.5 or between 247.5 and 292.5, we  
 113 refer to the movement as *orthogonal*. Of course, this partitioning of the turning circle can be varied and the  
 114 sensitivity of results to this partition evaluated.

## 115 2.2. Individual behavior

116 We first focus on the movement of an individual A, though in the context of individual B, as represented  
 117 by that time values **headA**( $t$ ), **dirAB**( $t$ ), and **diffA**( $t$ ). We begin by identifying the following three behavioral  
 118 modes (Fig. 1, with examples shown in Fig. 2):

119 (a) A approaches B: blue segments in Fig. 1

120 (b) A retreats from B: red segments in Fig. 1

121 (c) A moves orthogonally to B (i.e., around 90 or 270 degrees): purple segments in Fig. 1

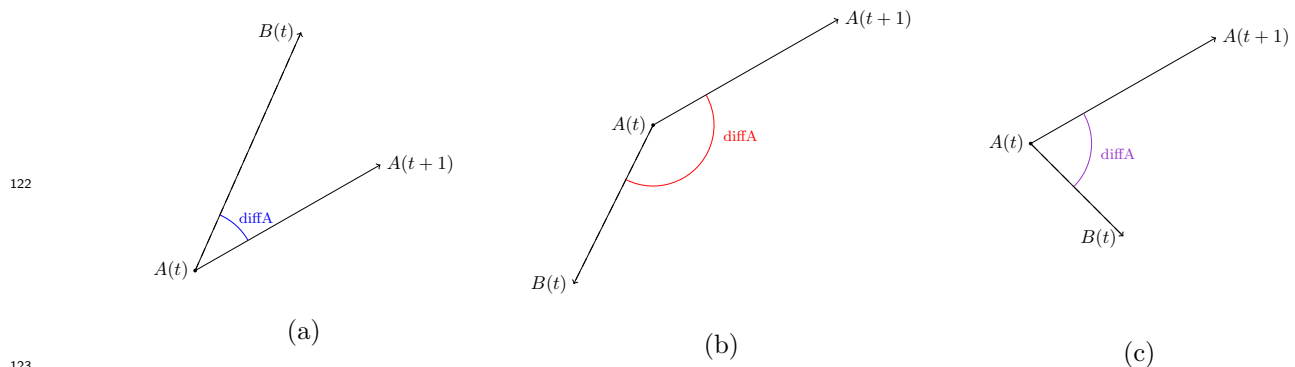


Figure 2: Example of behaviour classification for individual A: (a) approach, (b) retreat, (c) orthogonal individual behaviour, in relation to individual B.

125 In particular, we are interested in how these approach, retreat and orthogonal modes may depend on the  
126 distance between A and B, as well as influenced by temporal (diurnal, seasonal) and local environmental  
127 (landscape features, other individuals present, weather conditions, etc.) factors. Thus, in the first instance,  
128 we bin the classification of individual behaviors in relation to the distance between pairs of individuals.  
129 Specifically, for each individual in the dyad and for each chosen distance interval, we count the number of  
130 points at which approach, retreat and orthogonal movements are detected. We then evaluate whether or not  
131 the proportion of approaches to retreats are significantly different from random: given the symmetry of the  
132 problem, once the orthogonal movement points are removed, this proportion should be not be significantly  
133 different from 0.5. If it is, we can conclude that individual A's behavior with respect to be B is one of  
134 approach or retreat, as the case may be.

135 However, it is important to note that in the case where the number of retreats and approaches do not differ  
136 significantly from each other, they may still differ from random once the orthogonal points have been taken  
137 into account. Essentially, in this case we can conclude that approach and retreat behaviors, though they  
138 may be equally likely, are directed and hence intended when they occur. Thus the analysis when orthogonal  
139 movement designations are considered can be used to see to what extent approach and retreat behaviors are  
140 directed. Note that the larger the purple area in Fig. 1 the more the movement points are directed when  
141 the approach or retreat points are significantly different from random.

### 142 2.3. Dyadic behaviour

143 Our method also includes the identification of dyadic behavioral modes beyond the classification of how  
144 individuals move with respect to one another. In particular, at matching points for each dyad, we assign

145 one of the following six dyadic modes of behavior:

1. both individuals approach each other
2. both individuals retreat from each other
3. one individual approaches while the other individual retreats
- 146 4. one individual moves orthogonally, the other approaches
5. one individual moves orthogonally, the other retreats
6. both individuals move orthogonally

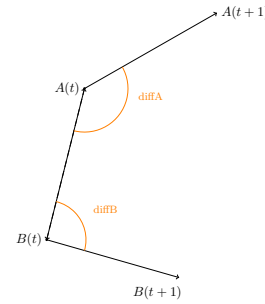


Figure 3: **diffA** and **diffB**: angle difference between the absolute and the relative headings for individuals A and B respectively.

147 As with the individual behavioral modes, we can use sample sizes and the expected proportions of each of  
148 the behavioral modes to assess whether or not a particular dyadic mode occurs significantly more often than  
149 expected at random over a particular set of intervals of time or in particular locations on the landscape.  
150 Specifically, if we exclude dyadic time-matched points at which one of the individuals is moving orthogonally,  
151 we expect the proportion of modes 1-3 to be 0.25, 0.25 and 0.5—the latter when the roles of A and B are  
152 interchangeable. Otherwise, we expect the proportion to all be equal to 0.25 if we consider mode 3 in the  
153 context of “A approaches while B retreats” compared with “A retreats while B approaches.”

#### 154 2.4. *Extended analysis involving absolute headings and relative speed*

155 We build on the previous analysis to extract dyadic behaviour such as *A following B* or *A and B walking side*  
156 *by side*. To achieve this, we consider also the *relative speed* of the individuals in the pair and the difference  
157 between their *absolute headings*. The speed of an individual at a particular point is calculated in terms of its  
158 distance to the next consecutive point, for all its relocation points before these points are time matched with  
159 the other’s points, as described above. Time-matched points then inherit the speed calculation associated  
160 with each of these matched points. We then categorize the *relative speed* of a dyad (A,B) as *similar speed*, *A*  
161 *faster than B* or *B faster than A*. To each of the six dyadic modes described in the previous section, we can  
162 now assign an additional designator: a.) similar speed, b.) A faster than B, 3.) B faster than A. This yields a  
163 total of 18 dyadic movement modes: 1a, 1b, ..., 6c. This additional designator, combined with the following  
164 heading analysis, will give us the opportunity to extract specific behaviours of interest, as elaborated in  
165 Section 3.3. In the SOF, we provide a table with all the dyadic movement modes and the description of the  
166 behaviours of interest.

167 For an *a priori* threshold value  $\theta$  (which may vary in a sensitivity analysis of results to this parameter value)

168 in the context of individual headings, we classify a dyad as having a *similar heading* if the absolute value  
169 of the difference is below  $\theta$  or above  $360 - \theta$  (shown in cyan in Fig. 4), while we classify it as having *the*  
170 *opposite heading* if the difference lies between  $180 - \theta$  and  $180 + \theta$  degrees (shown in orange in Fig. 4).

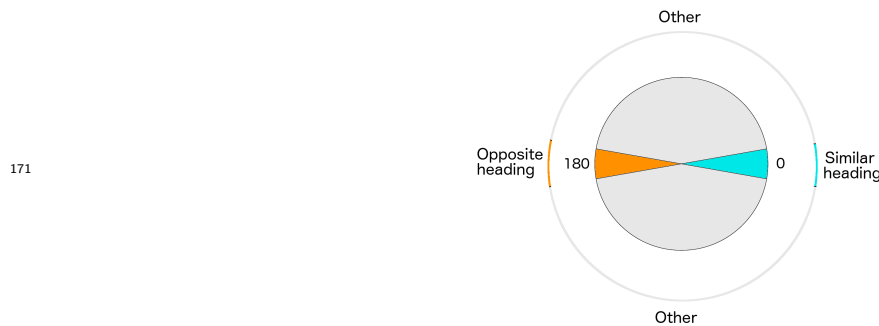


Figure 4: Heading difference for a dyad where, in this case, the angle  $\theta$  referred to in the text is 10 degrees. Cyan values are classified as a similar heading dyad, orange values as an opposite heading dyad, with all other cases shown in gray.

174 Given this additional classification, we can now combine all the different information—the dyadic behaviour,  
175 the relative speed and the heading difference—to extract behaviour of interest and compare its frequency of  
176 occurrence to that of other behaviours or, if desired, values expected at random. We can also compare the  
177 frequencies of the behaviours of interest, looking at difference among seasons, sex-type of individuals in the  
178 pair, or time of the day. For example, we may be interested in the following behaviour types:

- 179 • *Following behaviour*: dyadic behaviour of type 3a (dyadic behaviour of type 3, similar speed) and  
180 similar heading.
- 181 • *Side by side movement*: dyadic behaviour of type 6a (dyadic behaviour of type 6, similar speed) and  
182 similar heading.

183 These behaviours refine the previous dyadic behaviour of type 3 and 6, where the individuals also have  
184 similar speed and similar absolute heading.

## 185 2.5. Implementation

186 We perform this novel analysis using the R programming language, through the integrated development  
187 environment RStudio, and different R packages. We used the function `bearing` and the function `distm` from  
188 the R package `geosphere` to calculate the angles and the dyadic distance respectively; we used the function  
189 `binom.confint` from the R package `binom` to obtain the confidence intervals. Since the function `bearing`  
190 allows us to calculate the angle between the North direction and a given vector, expressed with longitude and  
191 latitude coordinates, the calculation of the angle `diffA`, between the two vectors shown in Fig. 1, was defined



192 as the difference between the absolute (headA) and relative (dirAB) heading, as described in Section 2.1.  
 193 Algorithm 1 describes the analysis of individual behaviour for both individual A and B, while the procedures  
 194 for dyadic and extended analysis are provided in the SOF. For the sake of simplicity, we assume that the  
 195 trajectories have location points that were recorded at almost the same time or have been interpolated to  
 196 match up in time.

---

**Algorithm 1:** Individual behaviour analysis

---

```

Input  $\mathcal{T}_A, \mathcal{T}_B, \mathcal{I}$ 
 $M_A = M_B = list()$ 
for  $i$  in  $\{1, \dots, n\}$  do
     $M_A[i] = M_B[i] = v_0(3)$ 
 $I_{AB} = T_A \cap T_B$ 
for  $t$  in  $I_{AB}$  do
    headA =  $f(A(t), A(t + 1))$ , headB =  $f(B(t), B(t + 1))$ 
    dirAB =  $f(A(t), B(t))$ , dirBA =  $f(B(t), A(t))$ 
    diffA = |headA - dirAB|, diffB = |headB - dirBA|
     $d_{AB} = d(A(t), B(t))$ 
    if  $\exists i : d_{AB} \in I_i$  then
         $m_A = f_c(\text{diffA})$ 
         $m_B = f_c(\text{diffB})$ 
         $M_A[i] = u(m_A, M_A[i])$ 
         $M_B[i] = u(m_B, M_B[i])$ 
return  $M_A, M_B$ 
    
```

---

197 The required inputs for the individual behaviour analysis are the trajectories for individual A and B ( $\mathcal{T}_A$  and  
 198  $\mathcal{T}_B$ ), and the  $n$  distance intervals  $\mathcal{I} = \{I_1, \dots, I_n\}$  used to bin the results. We use the lists  $M_A$  and  $M_B$  to  
 199 record the counts related to the different individual behaviour types and to the different  $n$  distance intervals.  
 200  $M_A$  and  $M_B$  are initiated as lists of  $n$  vectors, indicated with  $v_0(3)$ , which are vectors of length 3 and entry  
 201 all equal to 0. Each of these vectors is used to keep track of the counts for each of the 3 behaviour types for  
 202 the  $n$  different distance intervals.

203 The algorithm then calculates the set  $I_{AB}$ , the intersection between the time point sets  $T_A$  and  $T_B$ , thereby  
 204 identifying the sets of time points in both trajectories  $\mathcal{T}_A$  and in  $\mathcal{T}_B$ . For each of points in  $I_{AB}$ , the procedure  
 205 evaluates the three different angles for each individual: the function  $f$  calculates the angle between the  
 206 North direction and either the absolute heading vector (angles: headA and headB) or the relative heading  
 207 vector (angles: dirAB and dirBA). The algorithm then calculates the angles *difference* diffA and diffB, as  
 208 well as the distances  $d_{AB}$ . If  $d_{AB}$  lies within any of the chosen distance intervals  $I_i$ , then the algorithm  
 209 proceeds by classifying the angle *difference* as shown in Fig. 1 through the function  $f_c$ . The function  $u$   
 210 then updates the lists  $M_A$  and  $M_B$ , as a function of the angle classification and the corresponding distance

211 interval  $I_i$ . The outputs of this procedure are the lists  $M_A$  and  $M_B$ , which are used to construct barplots  
 212 and perform the statistical analysis. In particular, the statistical analysis uses the entries corresponding  
 213 to the approach and retreat behaviours for the calculation of the confidence intervals related to each  $I_i$ .  
 214 The R code for this analysis, the dyadic behaviour and the extended analysis can be found at [https:](https://ludovicalv.github.io/Dyadic_behaviour_method/)  
 215 [//ludovicalv.github.io/Dyadic\\_behaviour\\_method/](https://ludovicalv.github.io/Dyadic_behaviour_method/).

## 216 2.6. Simulated data

217 To validate our individual and dyadic methods of analysis, we applied them to simulated data with known  
 218 properties to see how well our methods could capture these properties. Our simulation models were con-  
 219 structed using the Numerus Model Builder (NMB) platform (Getz et al., 2018). These NMB models and simu-  
 220 lations used in the analysis can be found at [https://ludovicalv.github.io/Dyadic\\_behaviour\\_method/](https://ludovicalv.github.io/Dyadic_behaviour_method/).  
 221 Beyond providing test data for this study, our NMB relative-motion, biased random-walk (RM-BRW), as  
 222 described below, can also be used to explore theoretical question or help design empirical studies. For exam-  
 223 ple, our simulator can be used to evaluate how easily behaviors of different durations can be detected with  
 224 data collected at particular frequencies. This information would then inform the choice of data collection  
 225 frequency, battery use, or collar deployment. Additionally, our simulator can be used to test how sensi-  
 226 tive different algorithms may be to detecting movement path structures that have been defined at various  
 227 spatio-temporal scales (Getz et al., 2020).

228 To generate the set of simulated data used to validate our novel method, we model a relative-motion, biased  
 229 random-walk (RM-BRW) model with approach and retreat circumferences. In particular, for distances less  
 230 than  $d_R$ , A and B repulse one another, between  $d_R$  and  $d_I$  they attract one another and above  $d_I$  they behave  
 231 independently. Additionally, the approach and retreat behaviours only occur at each time step with a given  
 232 probability  $p_{\text{eff}}$  and with noise introduced by a coefficient  $\rho \in [0, 1]$ . A complete mathematical description  
 233 of the model is provided in our SOF. The NMB modelling panel is shown in Fig. 5.

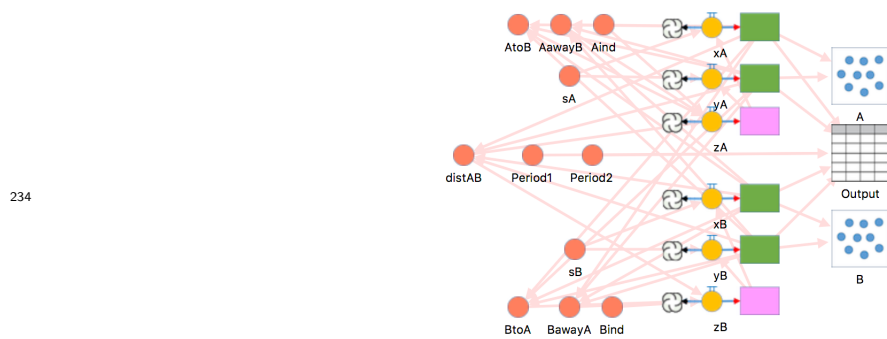


Figure 5: NMB panel: RM-BRW model

235 We also extended the model to include a time-dependent component to the attraction and repulsion be-  
236 haviour. Specifically, we allowed attraction to operate only during the first quarter of the day, repulsion  
237 during the second quarter of the day, and independent movement for the remaining half day.

### 238 *2.7. Empirical data*

239 We applied our method to GPS relocation data from 39 African elephants, collected between 2008 and 2015  
240 in Etosha National Park, Namibia (Abrahms et al., 2017, Tsalyuk et al., 2019). The intervals at which these  
241 data were recorded varied among 4, 3 and 2 points per hour (10, 15, and 14 individuals respectively). As  
242 mentioned in Section 2.1, these data collection frequencies are commonly reported in the GPS movement  
243 literature. Data were collected over different periods ranging from 2.5 months to 4.5 years. The time line of  
244 data collection for each individual and for each different frequency is provided in our SOF.

## 245 **3. Results**

### 246 *3.1. Simulations*

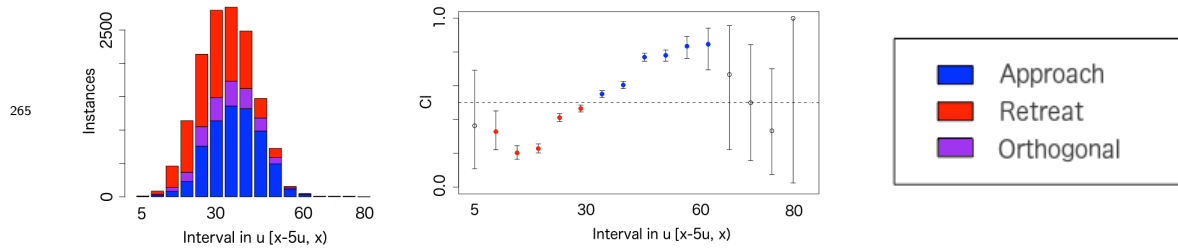
247 We simulated paths for A and B over a 10 day period, using a time step of 1 minute. Our unit spatial measure  
248 was set to 10 m and the repulsion and attracting circle diameters were set to  $d_R = 30$  and  $d_I = 60$  (i.e.,  
249 300 and 600 m respectively). The results reported in the first two subsections are for the time-independent  
250 version of the model, while those reported in the third subsection are for the time-dependent version of the  
251 model.

#### 252 *3.1.1. Individual behaviour*

253 To show the distribution of the three different individual behaviour types, we use barplots and the 3-colours  
254 legend introduced in Section 2.1 (Fig. 1). Specifically, we identified and binned the frequencies of approach,  
255 retreat and orthogonal behaviours using equal-width classes of pair distance, starting with a 0-5 unit bin and  
256 ending with a 75-80 unit bin, as shown in Fig. 6. Note that here we classify these approach/retreat/orthogonal  
257 behaviours per individual, with the results for the dyad as a whole reported in the next subsection.

258 In Fig. 6 (left panel) we show the results for individual A only, since individuals A and B are symmetric in the  
259 model (see SOF for further details). In addition, in Fig. 6 (central panel), we display the ratio between the  
260 approach count and the total of the approach and retreat counts, and the calculated 95% confidence intervals  
261 for each distance interval. We colored the results that are significantly larger than 0.5 in blue (approach) or  
262 less than 0.5 in red (retreat). As expected, we observe more retreats (red) for smaller distances, while the

263 number of approaches (blue) increases with pair distance. Since we set  $d_I = 60$  the pair distance tends to  
 264 remain below  $d_I$  most of the time.



266 Figure 6: Analysis barplot for individual A (left). Estimated confidence intervals (CI) for individual A, colored if showing a statistically significant result (center), according to the legend (right).

267 As introduced before, in this particular example  $d_R$  was chosen to be equal to 30 and  $d_I$  equal to 60 units.  
 268 We evaluate the statistical analysis results for the distance intervals:  $[0,30)$ ,  $[30,60)$  and  $[60,80)$ . We provide  
 269 the results of this analysis in Table 1, where we indicate statistically significant results above 0.5 (approach)  
 270 or below 0.5 (retreat) according to the results. As expected, we observe that for distance below 30 units, the  
 271 results are statistically significant and show retreat behaviour, while for distance in  $[30,60)$  the results show  
 272 approach behaviour. We do not observe a high number of instances and any statistically significant results  
 273 for distance above 60 units.

Individual	Distance interval (units)	Total	Approach	Lower CI	Upper CI	Approach	Retreat
A	$[0,30)$	5779	2236	0.3743	0.3996		✓
B		5821	2196	0.3648	0.3899		✓
A	$[30,60)$	6744	4311	0.6276	0.6507	✓	
B		6798	4367	0.6309	0.6538	✓	
A	$[60,80)$	24	12	0.2912	0.7088		
B		16	10	0.3543	0.848		

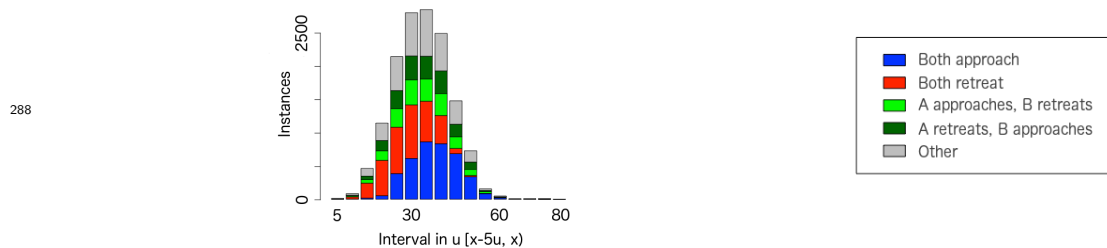
275 Table 1: Results of the individual analysis. We report the results grouped by distance intervals, providing the number of approaches and considering the total number of approach and retreat behaviours. We then show the bound of the confidence interval (CI) and check the result that are statistically significant at the 95% level.

### 276 3.1.2. Dyadic behaviour

277 By considering the behaviour of both individuals A and B, we compute the number of incidences of dyadic  
 278 type 3 mode of behavior separately for A and B: viz.,

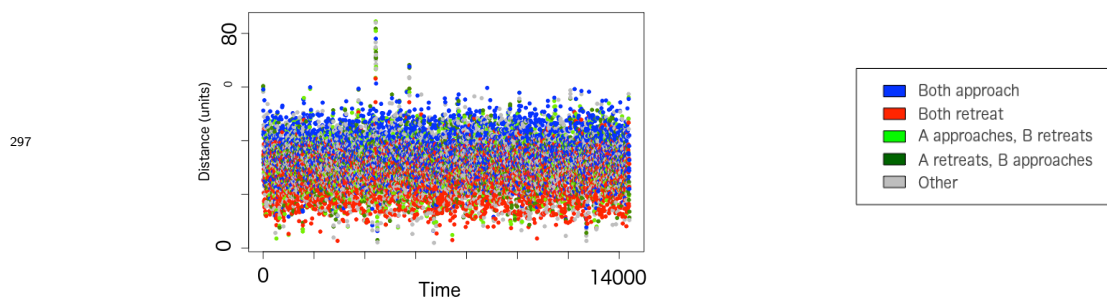
- 279 • 3(A,B): individual A approaches while individual B retreats
- 280 • 3(B,A): individual A retreats while individual B approaches

281 We also compute the number of instances of dyadic type 1 and 2 behaviors and exclude cases where orthogonal  
282 movements are involved (types 4-6). Our expectation, under a purely random movement hypothesis, is that  
283 each of these four instances (1, 2, 3(A,B), 3(B,A)) should occur with frequency 0.25. The number of  
284 instances of the various modes is illustrated in the barplot shown in Fig. 7, while the statistical analysis of  
285 the significance of the deviations from 0.25 at the various distances can be found in the table in SOF. As  
286 expected retreats occur significantly more often than random below 300 m (30 units) while approaches occur  
287 significantly more often than random between 300 and 600 m (30-60 units).



288 Figure 7: Analysis barplot for pair behaviour with legend provided on the right. We note that we observe significantly more  
289 than expected retreat behaviours (red) for distance below 30 (300 m), and significantly more approach behaviours than expected  
290 (blue) for distances above 30.

290 The results present in this and the previous subsection individuates that our method extracts the expected  
291 deviations from random that are a result of the biases that we have built into our model in terms of retreating  
292 behavior at  $<30$  units and attracting behaviour at  $>30$  units. Our analysis also allows to observe dyadic  
293 behaviour over time. For instance, in Fig. 8, we show the pair distance, coloring each point in time with  
294 the color corresponding to the dyadic behaviour type. We observe mostly red points at shorter distances,  
295 where the retreat behaviours predominate, and mostly blue points at larger distances, where the approach  
296 behaviours predominate.



297 Figure 8: Distance between the pair (left), colored according to the dyadic behaviour type as shown in the legend (right). Also  
298 in this case, we observe mostly retreat behaviours (red) for shorter distance while mostly approach behaviours (blue) for bigger  
distances.

299 *3.1.3. Time-dependent case*

300 In the case of the time-dependent model, we observe (Fig. 9) as expected that during the repulsion period  
301 both individuals move away from each other (indicated in red), while during the attraction period they both  
302 move towards each other (indicated in blue). When the individuals move independently we observe a less  
303 substantial change of the pair distance. A distance-dependent behaviour analysis across all time is not be  
304 able to capture the temporal patterns. By subdividing the data according to time of the day, however, we  
305 are able to observe time-dependent behaviour patterns, as documented in our SOF.

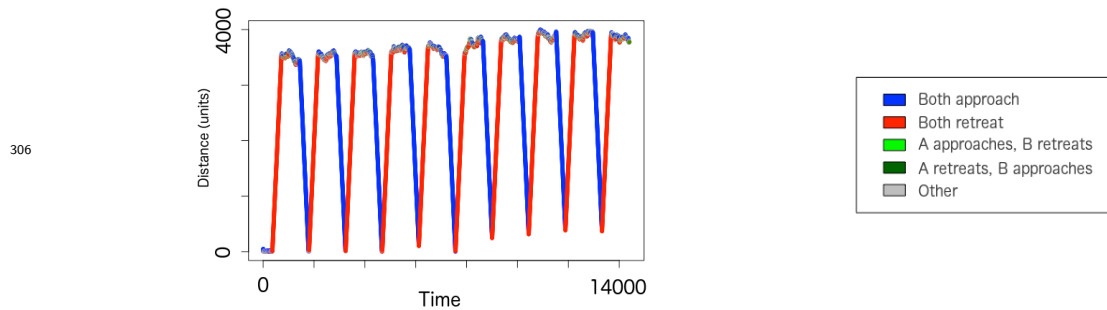


Figure 9: Distance between the pair (left), colored according to the dyadic behaviour type as shown in the legend (right). We observe that the distance between individuals increases with retreat behaviour (red) and decreases with approach (blue).

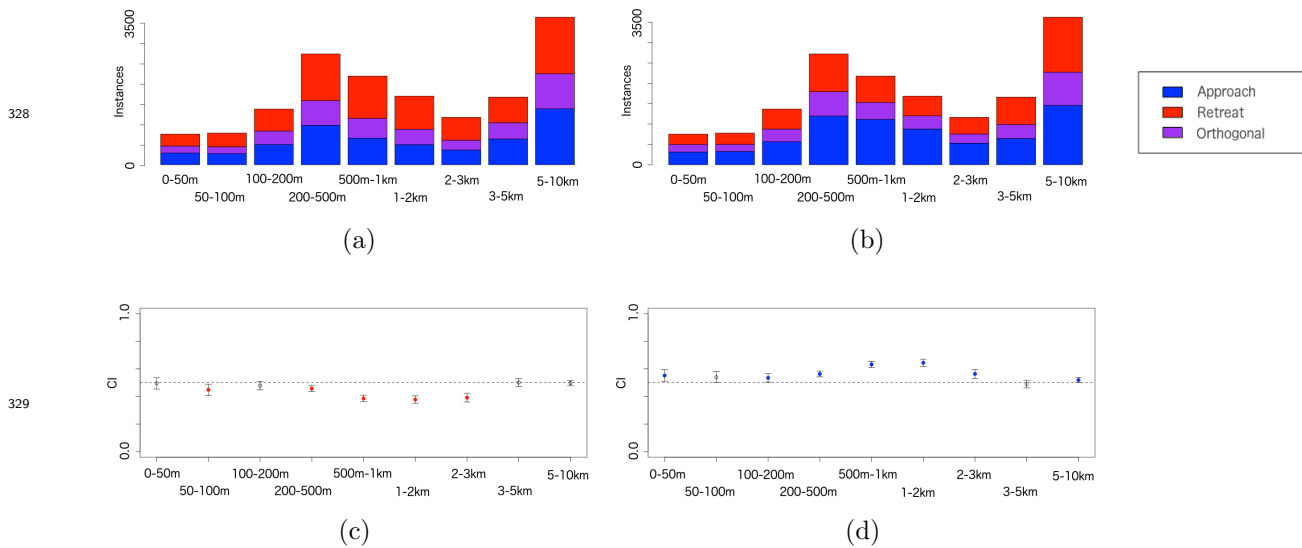
308 *3.2. Empirical results*

309 We first identified among the full set of elephant data those dyads that had matching frequencies within  
310 overlapping time periods and were close enough to one another for our method to yield interpretable results.  
311 In particular, we selected dyads that presented at least 500 instances at a distance below 1 km and had  
312 matching frequencies. In the first subsection below, we present the analysis results for a specific female-male  
313 dyad of interest. The male of this chosen pair had been tagged (Tsalyuk et al., 2019) as “with breeding  
314 herd” of the female. Given the repeated interactions, it is likely that the male was the son of one of the  
315 females in the same herd. In subsection 3.2.3, we provide a general overview of the results for all pairs that  
316 fit our matching criteria.

317 *3.2.1. Individual behaviour*

318 As presented in Section 3.1.1, we use barplots to show the distribution of the three different individual  
319 behaviour types, grouped by pair distance. In this case, we identified and binned the frequencies of approach  
320 and retreat behaviours using 9 different size classes, starting with a 0-50 m bin and ending with a 5-10 km  
321 bin, as shown in Figs. 10a and b. In addition, in Fig. 10c and d, we show the value of the ratio between

322 the approach count and the total of approach and retreat counts, and the calculated confidence intervals.  
 323 These results were colored if statistically significant: in blue for approach and in red for retreat individual  
 324 behaviour. We provide the values of the analysis in Table 2, where we indicate statistical significant results  
 325 (approach and retreat) with a check mark. We observe that the female retreats (Figs. 10a and c) significantly  
 326 more often than random at distances between 50m-3 km while the male approaches significantly more often  
 327 than random at distances < 3 km.



329 Figure 10: Individual behaviour classification for female (a) and male (b) and legend (right). Estimated CI, colored if providing  
 330 statistically significant results, for female (c) and male (d). We can observe that the female presents mostly retreat behaviours  
 (in red) while the male mostly approach behaviours (in blue).

331

Ind. in the pair	Distance interval (m)	Total	Approach	Lower CI	Upper CI	Approach	Retreat
Female	[0,50)	584	289	0.4536	0.5362		
Male		567	313	0.51	0.5935	✓	
Female	[50,100)	613	275	0.4088	0.489		✓
Male		603	326	0.4999	0.581		
Female	[100,200)	1040	498	0.4481	0.5097		
Male		1060	567	0.5043	0.5653	✓	
Female	[200,500)	2115	967	0.4358	0.4787		✓
Male		2125	1197	0.5419	0.5845	✓	
Female	[500,1000)	1691	653	0.3629	0.4098		✓
Male		1763	1115	0.6094	0.655	✓	
Female	[1000,2000)	1308	494	0.3513	0.4046		✓
Male		1361	877	0.6183	0.6698	✓	
Female	[2000,3000)	924	362	0.3601	0.4241		✓
Male		938	529	0.5315	0.596	✓	
Female	[3000,5000)	1266	635	0.4737	0.5295		
Male		1319	646	0.4625	0.5171		
Female	[5000,10000)	2764	1375	0.4787	0.5163		
Male		2809	1458	0.5004	0.5377	✓	

332 Table 2: Results of the individual analysis for female and male. We report the results grouped by distance intervals, providing the  
 333 total number of approach and retreat behaviours and the number of approach ones. We then show the bound of the confidence  
 interval (CI) and if the result was statistically significant showing approach or retreat behaviours. Approach behaviours are  
 334 mostly shown by the female while the male shows mostly retreat behaviours.

### 3.2.2. Dyadic behaviour

The results of our behavior analysis of our focal dyad is depicted in Fig. 11. We indicate statistically significant results (if above 0.25) in the upper part of the figure, corresponding to the different distance intervals, using the colors representing the different dyadic behaviour types. The table showing the results of the analysis is provided in our SOF. We observe that the statistically significant results correspond to pair behaviours of type 3(A,B) and 3(B,A). In particular, the most common pair behaviour corresponds to the female retreating while the male approaches (dyadic behaviour of type 3(B,A), A: female, B: male).

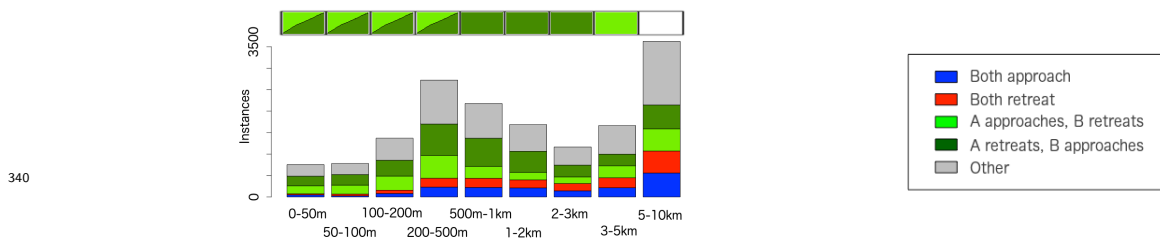


Figure 11: Analysis barplot for dyadic behaviour (right). The section above the barplot shows which of the four behaviours was significantly greater than 0.25 (when ignoring other), using the legend colors; two colored triangles were used if both behaviours of type 3 were statistically significant.

In Fig. 12 we show the results partitioned by season: hot-wet (Jan-Apr), cold-dry (May-Aug) and hot-dry (Sep-Dec). The hot-wet and hot-dry seasons contain significantly more female retreats from male interactions than the cold-dry season. Further, the hot dry period contains significantly more than random interactions at distances  $< 0.5$  km where male retreats while female approaches, and female retreats while male approaches at distances up to 10 km (tables detailing these results are presented in the SOF, as well as the pair distance showing the various dyadic behaviour types over time).

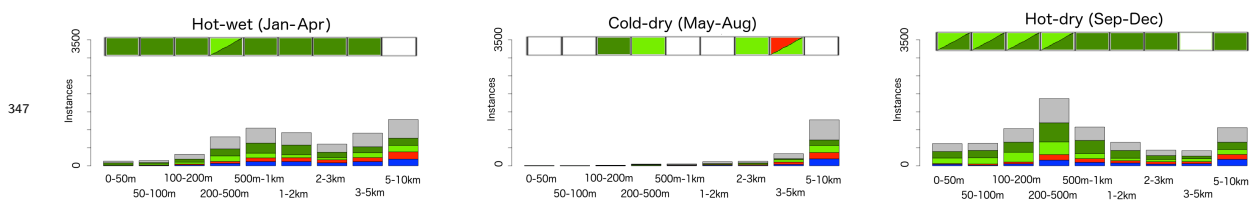


Figure 12: Analysis barplot for dyadic behaviour for hot-wet, cold-dry and hot-dry seasons. Same information above the barplots and same legend as Figure 11.

### 3.2.3. Analysis of pair of interest - dyadic behaviour

From the GPS data of the 39 individuals, we extracted 53 pairs of interest which satisfied the criteria mentioned in Section 3.2. The 15-min frequency data were collected from 10 male individuals and we extracted 17 male-male dyads of interest, while the 30-min data were collected from 14 female individuals and



353 we extracted 13 female-female dyads. The 20-min data were collected from 7 male and 8 female individuals:  
 354 the 23 pairs chosen from this data were 11 male-male, 5 male-female and 7 female-female. The data did  
 355 not provide information such as age of the individuals or any detailed relationship among them, except for  
 356 the information regarding the breeding herd of the female-male dyad presented in previous sections. More  
 357 informative data would have allowed a more extensive comparison among dyads.  
 358 We performed statistical analyses for the extracted dyads, and provide the percentage of dyads for which  
 359 the results were statistically significant (below and above 0.25), for each distance interval, in Table 3.  
 360 The detailed results for each data group are provided in our SOF. As shown in Table 3, the statistically  
 361 significant results (above 0.25) are related to behaviours of type 3(A,B) and 3(B,A) (A approaches while B  
 362 retreats and vice versa). In our SOF we also report the different percentage related to different sex-state pairs  
 363 of the 20-min frequency, observing prevalent retreats for females and approaches for males in female-male  
 364 dyads.

Distance interval	Both approach		Both retreat		A approaches B retreats		A retreats B approaches	
	Below 0.25	Above 0.25	Below 0.25	Above 0.25	Below 0.25	Above 0.25	Below 0.25	Above 0.25
[0m,50m)	36	6	70	0	0	51	2	57
[50m,100m)	51	0	58	0	0	58	2	40
[100m,200m)	68	0	68	0	0	64	2	51
[200m,500m)	77	0	74	0	0	77	2	62
[500m,1km)	62	0	34	0	4	51	9	49
[1km,2km)	55	0	43	0	13	53	11	34
[2km,3km)	30	0	17	4	9	28	15	32
[3km,5km)	9	15	13	4	23	15	11	26
[5km,10km)	9	23	26	17	21	25	28	17

Table 3: Analysis results for the pairs of interest. We observe that statistically significant results (above 0.25) are associated with behaviour of type 3 (one individual approaches while the other retreats). We colored the table cells according to the values: the darker cells contain higher values.

365

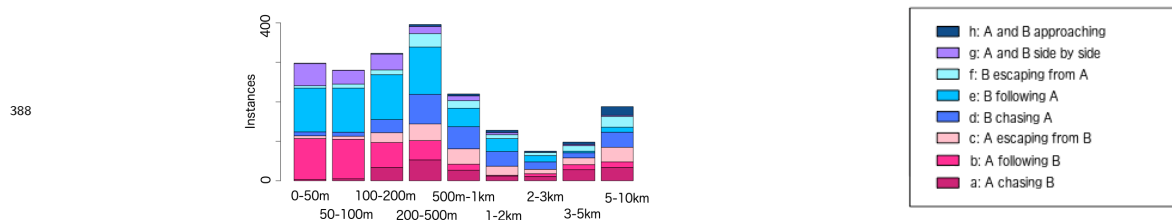
### 366 3.3. Extended analysis: female-male dyad

367 We performed an extended analysis that includes the absolute heading difference and relative speeds of the  
 368 individuals for the focal female-male pair discussed in sections 3.2.1 and 3.2.2. We focus on the following  
 369 eight behaviour modes, where A is the female and B the male:

- 370 a. A chasing B: A and B dyadic behaviour of type 3(A,B), speed of A greater than speed of B, similar  
 371 heading

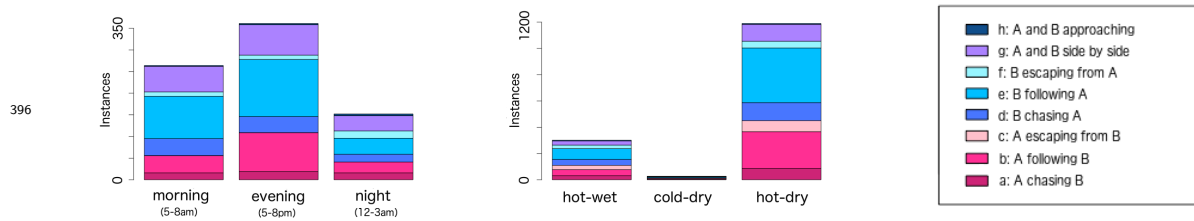
- 372 b. A following B: A and B dyadic behaviour of type 3(A,B), similar speed, similar heading
- 373 c. A escaping from B: A and B dyadic behaviour of type 3(B,A), speed of A greater than speed of B,  
374 similar heading
- 375 d. B chasing A: A and B dyadic behaviour of type 3(B,A), speed of B greater than speed of A, similar  
376 heading
- 377 e. B following A: A and B dyadic behaviour of type 3(B,A), similar speed, similar heading
- 378 f. B escaping from A: A and B dyadic behaviour of type 3(A,B), speed of B greater than speed of A,  
379 similar heading
- 380 g. A and B side by side: A and B dyadic behaviour of type 6, similar speed, similar heading
- 381 h. A and B approaching at a similar speed: A and B dyadic behaviour of type 1, similar speed, opposite  
382 headings

383 We categorize the relative speed of A (female) with respect to B (male) in proportional terms. Specifically,  
384 if the proportion exceeds  $\frac{3}{2}$ , we categorize the speed of A as *greater* than B, while if below  $\frac{2}{3}$  the speed of B  
385 is categorized as *greater* than A. Between these two proportions, we define that the two speeds as *similar*.  
386 In Fig. 13, we observe that the following behaviours (behaviours of type b and e) are the most common for  
387 the female-male pair of interest, especially for shorter distance between the individuals.



389 Figure 13: Results of the extended analysis. The legend is provided on the right, where A is the female and B the male. We observe that the following behaviours (type b and e) are the most frequent behaviours.

390 We also compared the frequencies of behaviours across diurnal and seasonal cycles, considering just data  
391 points for pair distances below 1 km. In Fig. 14 we depict the frequency of these behaviours at different  
392 times of the day (morning: 5-8am, evening: 5-8pm, night: midnight-3am) and for the different seasons. We  
393 observe that the frequency of interactions is relatively higher in the evening and substantially higher during  
394 the hot-dry season, but there are no outstanding differences among the different periods of the day and of  
395 the year in terms of the frequency of different behaviour types.



396 Figure 14: Extended analysis for dyadic behaviour types for different times of the day (left) and different seasons (center).  
397 Legend on the right. Also in this case, individual A corresponds to the female while individual B to the male.

#### 398 4. Discussion

399 The literature contains several reviews on methods developed to study dyadic interactions. Miller (2012), for  
400 example, explores how spatially explicit simulated data can be used to analyse dynamic interactions between  
401 individuals. He uses five different techniques to quantify dynamic interactions based on GPS data of pairs of  
402 individuals, using both real (brown hyenas dyads) and simulated data. On the other hand, Long et al. (2014)  
403 evaluate the efficacy of eight different dynamic interaction indices, using both simulated and empirical data.  
404 They partition these indices into point-based measures, which typically study approach/retreat behaviour,  
405 and path-based measures, which look at movement behaviour. In particular, the index of proximity in  
406 space and the coefficient of association, example of point-based measures, look at the proportion of close  
407 simultaneous locations over the total number, while the correlation index and the dynamic interaction  
408 index, example of path-based measures, respectively evaluate the correlation and cohesiveness of movement  
409 segments that connect consecutive locations. Joo et al. (2018), following Long et al. (2014), assess the  
410 adequacy of 12 metrics introduced in previous works to assess specific aspects of joint-movement behaviour  
411 (two individuals move together for the total or a partial portion of their paths), focusing on proximity  
412 and coordination (synchrony) in direction and speed. The comparison is performed by building different  
413 scenarios with different levels of proximity and coordination to assess the ability of the metrics to capture  
414 various features. Some of these indices were used in Eriksen et al. (2009) to study both static and dynamic  
415 interactions among wolves and moose, and in Tosa et al. (2014) to examine dyads of female white-tailed deer  
416 within and between groups and to understand how those may related to pathogen transmission.

417 These existing techniques are based on the analysis of simultaneous locations, with or without a pair distance  
418 threshold and permutations of these, to perform different studies by comparing, for example, mean distance  
419 between simultaneous and permuted locations (coefficient of sociality), or using the overlap of home ranges  
420 as part of the analysis (Minta's coefficient of interactions, half-weight association index). These dyadic

421 approaches focus primarily on pairings of animals in space and time, with distance thresholds determining  
422 when dyads form and number of GPS fixes determining the length of time of the dyadic interaction. These  
423 techniques provide valuable information on which individuals form dyads and when they begin and end.  
424 Our methodology expands on this by introducing direction of movement and positions of individuals while  
425 interacting as a dyad. Our approach is also based on the analysis of simultaneous locations and can be  
426 defined as a point-based measure. However, it introduces the novelty of classifying angles related to the  
427 direction of movement and the position of the other individual in the dyad. After this classification, our  
428 methodology uses pair distance to group and analyse the results so that a deeper understanding of approach  
429 and retreat behaviours can be obtained. Additionally, through our extended dyadic behaviour analysis, we  
430 are able to evaluate frequencies of different dyadic behaviours that include differences in speed and absolute  
431 headings of the individuals.

432 A method for identifying various combinations of attraction, avoidance, and neutrality, using a framework  
433 of step-selection functions and both simulated and empirical data, is presented in Schlägel et al. (2019). In  
434 this work attraction and avoidance are considered in terms of an individual choosing locations that other  
435 individuals respectively use or do not use, while neutrality relates to ignoring the location use of others. In  
436 contrast to our approach, this method considers the distance to the home-range centers and not between  
437 pairs. Additionally, it is more suitable for evaluating short-range interactions (because the considered steps in  
438 the step-selection function might not reach far enough), while our method can apply to interactions that take  
439 place over any relevant distance. Other studies that include the relevance of sex in dyadic interactions is one  
440 on grizzly bear pairs where Doncaster's measure (Doncaster, 1990) was used to understand sex-dependent  
441 and season-dependent interactions. Also, Spiegel et al. (2018) use a proximity-based social network method  
442 to analyse approach and retreat behaviours, with a specific focus on interaction rates between intrasex and  
443 intersex pairs.

444 Finally, a number of elephant interaction studies are reported in the literature. These include elephant-  
445 human interactions (Shaffer et al., 2019, Rossman et al., 2017), as well as zoo elephant tactile contact  
446 and proximity interactions (Bonaparte-Saller and Mench, 2018). Dyadic interactions among male African  
447 elephants (Goldenberg et al., 2014) and the social dynamics of female Asian elephants (de Silva et al., 2011)  
448 have also come under scrutiny, but these do not incorporate such movement elements as relative direction  
449 and speed that our methodology is specially designed to address.

## 450 **5. Conclusions**

451 In this paper we introduce a novel methodology to classify distance-dependent dyadic behaviour that allows  
452 us to extract approach and retreat behaviours by analysing animal GPS relocation data with matching  
453 frequencies and overlapping time periods. Our methodology was developed to classify distance-dependent  
454 behaviour, but it can be applied using other types of classification. We anticipate that our method will prove  
455 to be useful when applied to understanding behavioural persistence by analysing time series that capture the  
456 different behaviour types over time. In addition, it can be applied to investigating how different frequencies  
457 of data collection permit extraction of particular behaviours of interest at different spatio-temporal scales.  
458 It can also be embedded in studies that take various environmental factors, such as water sources or other  
459 types of resources, into account as covariates correlated with particular types of dyadic interactions.

## 460 **Acknowledgments and SOF File**

461 The development of NOVA, a precursor to Numerus Model Builder, was supported by NSF grant CNS-  
462 0939153 to Oberlin College and NSF-EEID grant 1617982 (PI: WMG). Wayne Getz is co-owner with two  
463 others of Numerus Inc., which provides a version of Numerus Modeler Builder online for free use. The  
464 collection of the GPS movement data were supported by grant NIH GM083863 (WMG, PI). In addition,  
465 LLV and JKB were funded by NIH 1R01GM117617-01 (PI: JKB). The supporting online file SOF, containing  
466 details of the model description and the analysis results is available at [https://ludovicalv.github.io/  
467 PDFs/Ellep\\_paper.pdf](https://ludovicalv.github.io/PDFs/Ellep_paper.pdf). The NMB models and the R code can be downloaded at [https://ludovicalv.  
468 github.io/Dyadic\\_behaviour\\_method/](https://ludovicalv.github.io/Dyadic_behaviour_method/).

## 469 **Data Accessibility Statement**

470 We agree to archive the data associated with this manuscript should the manuscript be accepted. We intend  
471 to use a Zenodo repository.

## 472 **Authors' contributions statement**

473 LLV and WMG conceived the study and developed the methodology, LLV analysed the data, and LLV, JKB  
474 and WMG contributed to the writing of the manuscript.

## 475 References

- 476 Abrahms, B., Seidel, D.P., Dougherty, E., Hazen, E.L., Bograd, S.J., Wilson, A.M., McNutt, J.W., Costa,  
477 D.P., Blake, S., Brashares, J.S., et al., 2017. Suite of simple metrics reveals common movement syndromes  
478 across vertebrate taxa. *Movement ecology* 5, 1–11.
- 479 Archie, E.A., Morrison, T.A., Foley, C.A., Moss, C.J., Alberts, S.C., 2006. Dominance rank relationships  
480 among wild female African elephants, *Loxodonta africana*. *Animal Behaviour* 71, 117–127.
- 481 Bonaparte-Saller, M., Mench, J.A., 2018. Assessing the dyadic social relationships of female african (*Lox-*  
482 *odonta africana*) and asian (*Elephas maximus*) zoo elephants using proximity, tactile contact, and keeper  
483 surveys. *Applied Animal Behaviour Science* 199, 45–51. [https://doi.org/10.1016/j.applanim.2017.](https://doi.org/10.1016/j.applanim.2017.10.011)  
484 [10.011](https://doi.org/10.1016/j.applanim.2017.10.011).
- 485 Breed, M.D., 2003. Nestmate recognition assays as a tool for population and ecological studies in eusocial  
486 insects: a review. *Journal of the Kansas Entomological Society* , 539–550.
- 487 Calenge, C., Dray, S., Royer-Carenzi, M., 2009. The concept of animals' trajectories from a data analysis  
488 perspective. *Ecological informatics* 4, 34–41.
- 489 Codling, E., Hill, N., 2005. Sampling rate effects on measurements of correlated and biased random walks.  
490 *Journal of Theoretical Biology* 233, 573–588.
- 491 Doncaster, C.P., 1990. Non-parametric estimates of interaction from radio-tracking data. *Journal of Theo-*  
492 *retical Biology* 143, 431–443. [https://doi.org/10.1016/S0022-5193\(05\)80020-7](https://doi.org/10.1016/S0022-5193(05)80020-7).
- 493 Erbe, C., Reichmuth, C., Cunningham, K., Lucke, K., Dooling, R., 2016. Communication masking in marine  
494 mammals: A review and research strategy. *Marine pollution bulletin* 103, 15–38.
- 495 Eriksen, A., Wabakken, P., Zimmermann, B., Andreassen, H., Arnemo, J., Gundersen, H., Milner, J., Liberg,  
496 O., Linnell, J., Pedersen, H., Sand, H., Solberg, E.J., Storaas, T., 2009. Encounter frequencies between  
497 GPS-collared wolves (*Canis lupus*) and moose (*Alces alces*) in a Scandinavian wolf territory. *Ecological*  
498 *Research* 24, 547–557. <https://doi.org/10.1007/s11284-008-0525-x>.
- 499 Getz, W.M., Luisa Vissat, L., Salter, R., 2020. Simulation and Analysis of Animal Movement Paths Using  
500 Numerus Model Builder, in: 2020 Spring Simulation Conference (SpringSim), pp. 1–12. [https://doi.](https://doi.org/10.22360/SpringSim.2020.TMS.001)  
501 [org/10.22360/SpringSim.2020.TMS.001](https://doi.org/10.22360/SpringSim.2020.TMS.001).

- 502 Getz, W.M., Salter, R., Muellerklein, O., Yoon, H.S., Tallam, K., 2018. Modeling epidemics: A primer and  
503 Numerus Model Builder implementation. *Epidemics* 25, 9–19. [https://doi.org/10.1016/j.epidem.](https://doi.org/10.1016/j.epidem.2018.06.001)  
504 2018.06.001.
- 505 Getz, W.M., Smith, K.B., 1986. Honey bee kin recognition: learning self and nestmate phenotypes. *Animal*  
506 *behaviour* 34, 1617–1626.
- 507 Goldenberg, S.Z., de Silva, S., Rasmussen, H.B., Douglas-Hamilton, I., Wittemyer, G., 2014. Controlling  
508 for behavioural state reveals social dynamics among male African elephants, *Loxodonta africana*. *Animal*  
509 *Behaviour* 95, 111–119.
- 510 Hulse, S.H., 2002. Auditory scene analysis in animal communication. *Advances in the Study of Behavior*  
511 31, 163–201.
- 512 Joo, R., Etienne, M.P., Bez, N., Mahévas, S., 2018. Metrics for describing dyadic movement: a review.  
513 *Movement ecology* 6, 26.
- 514 Long, J.A., Nelson, T.A., Webb, S.L., Gee, K.L., 2014. A critical examination of indices of dynamic inter-  
515 action for wildlife telemetry studies. *Journal of Animal Ecology* 83, 1216–1233.
- 516 McComb, K., Reby, D., Baker, L., Moss, C., Sayialel, S., 2003. Long-distance communication of acoustic  
517 cues to social identity in African elephants. *Animal Behaviour* 65, 317–329.
- 518 Miller, J.A., 2012. Using Spatially Explicit Simulated Data to Analyze Animal Interactions: A Case Study  
519 with Brown Hyenas in Northern Botswana. *Transactions in GIS* 16, 271–291. [https://doi.org/10.1111/](https://doi.org/10.1111/j.1467-9671.2012.01323.x)  
520 [j.1467-9671.2012.01323.x](https://doi.org/10.1111/j.1467-9671.2012.01323.x).
- 521 O’Connell-Rodwell, C.E., 2007. Keeping an “ear” to the ground: seismic communication in elephants.  
522 *Physiology* 22, 287–294.
- 523 Rossman, Z.T., Padfield, C., Young, D., Hart, L.A., 2017. Elephant-Initiated Interactions with Humans: In-  
524 dividual Differences and Specific Preferences in Captive African Elephants (*Loxodonta africana*). *Frontiers*  
525 *in Veterinary Science* 4, 60. <https://doi.org/10.3389/fvets.2017.00060>.
- 526 Schlägel, U., Signer, J., Herde, A., Eden, S., Jeltsch, F., Eccard, J., Dammhahn, M., 2019. Estimating  
527 interactions between individuals from concurrent animal movements. *Methods in Ecology and Evolution*  
528 <https://doi.org/10.1111/2041-210X.13235>.

- 529 Shaffer, L.J., Khadka, K.K., Van Den Hoek, J., Naithani, K.J., 2019. Human-elephant conflict: A review of  
530 current management strategies and future directions. *Frontiers in Ecology and Evolution* 6, 235. <https://doi.org/10.3389/fevo.2018.00235>.
- 531
- 532 Shorey, H.H., 2013. *Animal communication by pheromones*. Academic Press.
- 533 de Silva, S., Ranjeewa, A.D., Kryazhimskiy, S., 2011. The dynamics of social networks among female Asian  
534 elephants. *BMC ecology* 11, 17.
- 535 Spiegel, O., Sih, A., Leu, S.T., Bull, C.M., 2018. Where should we meet? Mapping social network interactions  
536 of sleepy lizards shows sex-dependent social network structure. *Animal Behaviour* 136, 207–215. <https://doi.org/10.1016/j.anbehav.2017.11.001>.
- 537
- 538 Tosa, M., Schaubert, E., Nielsen, C., 2014. Familiarity breeds contempt: Combining proximity loggers  
539 and GPS reveals female white-tailed deer (*Odocoileus virginianus*) avoiding close contact with neighbors.  
540 *Journal of wildlife diseases* 51. <https://doi.org/10.7589/2013-06-139>.
- 541 Tsalyuk, M., Kilian, W., Reineking, B., Getz, W.M., 2019. Temporal variation in resource selection of  
542 African elephants follows long-term variability in resource availability. *Ecological Monographs* 89, e01348.
- 543 Voelkl, B., Kasper, C., Schwab, C., 2011. Network measures for dyadic interactions: stability and reliability.  
544 *American Journal of Primatology* 73, 731–740.
- 545 Whitehead, H., Dufault, S., 1999. Techniques for analyzing vertebrate social structure using identified  
546 individuals. *Adv Stud Behav* 28, 33–74.
- 547 Wittemyer, G., Getz, W., 2007. Hierarchical dominance structure and social organization in African ele-  
548 phants, *Loxodonta africana*. *Animal Behaviour* 73, 671–681.